

## Charged Particle Penetration Distance and Mass Stopping Power Calculations on Some Nuclear Reactor Control Rod Materials

Mert ŞEKERCİ<sup>1\*</sup>, Hasan ÖZDOĞAN<sup>2</sup>, Abdullah KAPLAN<sup>1</sup>

<sup>1</sup>Süleyman Demirel University, Department of Physics, Isparta, 32260, Turkey

<sup>2</sup>Akdeniz University, Department of Biophysics, Antalya, 07070, Turkey

Geliş / Received: 09/05/2019, Kabul / Accepted: 24/07/2019

### Abstract

One possible solution to the increasing energy demand, which mankind has been facing through, might be pointed as the nuclear reactors that work with the fission mechanism. In order to pursue the operation of these facilities, many equipment have been designed in a way that all of them could operate together where the control rods could be given as one of the vital parts among them. Material properties of these components, such as physical-chemical characteristics and their behaviors under different interactions, have an undeniable importance. Due to that, gathering all the possible information about the materials used for the production of these components is extremely important. By considering this importance, in this study, the mass stopping power and charged particle penetration distance calculations have been done for some materials which have possible usage in nuclear reactor control rods using alphas, <sup>3</sup>He, tritons, deuterons and protons within the energy range of 1-50 MeV via employing two of the most known computer aided calculation and simulation software which are GEANT4 and MCNP. Obtained results from both codes have been visualized by graphing and compared with each other.

**Keywords:** Charged particle, Penetration distance, Mass stopping power; Reactor control rod material

## Bazı Nükleer Reaktör Kontrol Çubuğu Malzemelerinde Yüklü Parçacık Giricilik Mesafesi ve Kütle Durdurma Gücü Hesaplamaları

### Öz

İnsanlığın karşılaştığı artan enerji talebine olası bir çözüm, fisyon mekanizmasıyla çalışan nükleer reaktörler olarak gösterilebilir. Bu tesislerin çalışmalarını takip edebilmek için, aralarında hayati öneme sahip olarak gösterilebilecek kontrol çubuklarının da bulunduğu ve tamamı birlikte çalışabilecek şekilde tasarlanmış pek çok ekipman bulunmaktadır. Bu bileşenlerin fiziksel-kimyasal özellikleri ve farklı etkileşimlerdeki davranışları gibi malzeme özellikleri yadsınamaz bir öneme sahiptir. Bu nedenle, bu bileşenlerin üretiminde kullanılan malzemelerle ilgili olası tüm bilgilerin toplanması son derece önemlidir. Bu önem göz önünde bulundurularak bu çalışmada, nükleer reaktör kontrol çubuklarında kullanım olasılığı bulunan bazı materyaller için kütle durdurma gücü ve yüklü parçacık giricilik mesafesi 1-50 MeV enerji aralığındaki alfa, <sup>3</sup>He, triton, döteron ve protonlar için en çok bilinen bilgisayar destekli hesaplama ve benzetim programları olan GEANT4 ve MCNP kullanılarak yapılmıştır. Her iki koddan elde edilen sonuçlar grafiklerle görselleştirilmiş ve birbirleriyle kıyaslanmıştır.

**Anahtar Kelimeler:** Yüklü parçacık, Giricilik mesafesi, Kütle durma gücü; Reaktör kontrol çubuğu malzemesi

## 1. Introduction

Expanding cities, people's desire to have better living standards, industrial advancements and technological additions on which modern day-to-day life is growing on more and more have led an increase on the requested amount of energy, especially electricity energy (IAEA, 2017). The behavior on the use of conventional energy supply

methods to meet this growing energy demand may not be continuous or lead to irrational consequences due to the facts in the increase of carbon emission, efficiency concerns, sustainability and raw material status on natural sources, such as oil and natural gas. Due to that the use of nuclear reactors, which operates with the principle of fission mechanism and could be pointed as one of the most advanced technological and scientific

productions of our time, has become highly conceivable for the generation of electricity due to their respectable benefits such as reduction in the carbon emission, ability of continuously energy generation, better energy production performance and many more (Becker et al., 2008). Efforts to achieve better results in this field have led to the development of fission reactors in different types and characteristics that work with the fission mechanism which must be kept under control. All of the 452 (PRIS, 2019) reactors actively used for the energy generation on the day of reference have include many systems that play active roles in the operation of these facilities. Among these, the control rods can be shown as one of the most important components considering their influence and effect on controlling the fission reaction and relatedly the energy production continuity. For this reason, many studies have been made and still be doing for the selection of appropriate material to be used in the production of control rods (IAEA, 1995; IAEA, 1996; IAEA; 2000, Kalcheva and Koonen, 2007; Ashby and Smidman, 2010). Since these components will provide a control on the neutrons resulting from the fission mechanism, it may be considered that the primarily investigation topic should be the effects of neutrons on the materials used in their manufacturing. However, investigating the effects of the charged particles on the control rod materials in order to obtain the data for the material development studies as well as to create the material characteristic by knowing the response of the material in different interactions and thus to use them in various areas such as accelerator technologies, medical applications, shielding purposes, space applications and other scientific studies is also a very important issue. So, obtaining the material stopping power and the particle penetration distance values as a result of charged particle interactions on the materials may provide beneficial and useful results

which can be used in many scientific, technological and industrial applications. The existence of studies in this and similar context in the literature also shows the accuracy and importance of this statement (Tekin and Manici, 2017; Bozkurt and Sarpün, 2018a; Bozkurt and Sarpün, 2018b; Artun, 2018a; Artun, 2018b). In this study, with the motivation by considering the above mentioned importance, for the elements of Hafnium (Hf), Samarium (Sm), Europium (Eu), Gadolinium (Gd) and Dysprosium (Dy) also for the oxide compounds of these elements that are Hafnium(IV) oxide (Hafnia) ( $\text{HfO}_2$ ), Samarium(III) oxide (Samaria) ( $\text{Sm}_2\text{O}_3$ ), Europium(III) oxide (Europia) ( $\text{Eu}_2\text{O}_3$ ), Gadolinium(III) oxide (Gadolinia) ( $\text{Gd}_2\text{O}_3$ ) and Dysprosium(III) oxide (Dysprosia) ( $\text{Dy}_2\text{O}_3$ ), which have been considered and studied on the use of control rod production, the mass stopping power values on different charged particle interactions and the penetration distance values of these charged particles have been obtained (IAEA, 1995; IAEA, 1996; IAEA; 2000, Kalcheva and Koonen, 2007; Ashby and Smidman, 2010). Five different charged particle interactions on these materials have been investigated where the particles have been selected as alphas,  $^3\text{He}$ , tritons, deuterons and protons within the energy range of 1-50 MeV. Calculations have been carried out by employing two of the best known and frequently used computer aided simulation and calculation tools which are GEANT4 (Geometry And Tracking) (Agostinelli et al., 2003) and MCNP (Monte Carlo N-Particle) (Goorley et al., 2013). Obtained calculation results via both codes have been compared and the results have been graphed for better visual understanding.

## 2. Material and Method

The history of charged particle interaction with material goes many years back. Since then an equation which has been modified

many times and reconstructed by adding many correction terms, such as shell and density corrections, has been employing for resolving the energy loss mechanisms of the charged particles while they move within the substance. The so-called equation, which is

$$-\frac{dE}{dx} = KZ^2 \frac{Z}{A} \frac{1}{\beta^2} \left[ \frac{1}{2} \ln \frac{2m_e c^2 \beta^2 \gamma^2 T_{max}}{I^2} - \beta^2 - \frac{\delta(\beta\gamma)}{2} \right] \quad (1)$$

The unit of the stopping power depends on whether the energy loss in the unit length is associated with the number of atoms in the unit volume or unit mass. In the case of association with the number of atoms in the unit volume, the stopping power is expressed in the units of MeV/cm. However, in the case of association with the number of atoms in the unit mass, the energy loss in the unit g/cm<sup>2</sup> is

$$\left( \frac{1}{\rho} \frac{dE}{dx} \right) = 0.3071 \frac{Zz^2}{A} \frac{1}{\beta^2} \left[ 13.8373 + \ln \left( \frac{\beta^2}{1-\beta^2} \right) - \beta^2 - \ln(I) - \frac{\delta}{2} \right] \quad (2)$$

In the Eq. (2),  $A$  is the atomic mass of the absorber medium where  $z$  and  $Z$  are the atomic numbers of the incident particle and absorber medium, respectively.  $\beta$ , which is  $v/c$ , corresponds to the velocity of the incident particle and  $I$  is the mean excitation energy of the absorber medium. Among the parameters in Eq. (2),  $I$  is one of the most characteristic

$$I \approx \begin{cases} I_0 \cdot Z + I_C, & \text{if } Z < 13, I_0 = 12 \text{ eV}, I_C = 7 \text{ eV} \\ I_0 \cdot Z + I_C \cdot Z^{-0.19}, & \text{if } Z \geq 13, I_0 = 9.8 \text{ eV}, I_C = 58.8 \text{ eV} \end{cases} \quad (3)$$

The term  $\delta$  in Eq. (2) represents the density effect correction to the ionization loss. It is used to correct the dielectric polarization effects of the target material and it becomes more important for high energetic incident particles. With the increase of the incident particle energy, the velocity of the particle will increase too. As a result of this increment, the electric field of the particle will become flatter and more extended. Due to that electric field, the atoms along its path will be more prone to the polarization and so the polarization causes to the electric field

known as Bethe-Bloch equation (Bethe and Ashkin, 1953), also used to explain the mean rate of energy loss, in other words the stopping power of the material, and could be represented as given in Eq. (1) (Groom and Klein, 2000).

defined with the mass stopping power,  $S = -(1/\rho) dE/dx$ , and the unit will be MeVcm<sup>2</sup>/g. Eq. (1) can be rewritten as Eq. (2) for heavily charged particles, such as alpha, <sup>3</sup>He, triton, deuteron and proton, that also includes both soft and hard collision effects to express the mass stopping power (Attix, 1986).

parameter for the absorber medium. Evaluations for the  $I$  value have been generally obtained from the possible experimental measurements of the stopping power studies accomplished for protons, deuterons and alphas where the following empirical equations have been generated (Paul and Schinner, 2003).

shielding on the far electrons from the incoming particle. Consequently, less contribution to the overall energy loss mechanism will be provided due to the collisions generated with these shielded electrons rather than the Bethe-Bloch formula's prediction. For more dense materials, this effect will be increased because the polarization will be larger in these materials. To overcome this problem, density correction term is used which is generally calculated by using the Sternheimer's

parametrization given in Eq. (4) (Sternheimer et al., 1984).

$$\delta = \begin{cases} 2(\ln 10)x - \bar{C} & , x \geq x_1 \\ 2(\ln 10)x - \bar{C} + a(x_1 - x)^k & , x_0 \leq x < x_1 \\ 0 & , x < x_0 \text{ (nonconductors)} \\ \delta_0 10^{2(x-x_0)} & , x < x_0 \text{ (conductors)} \end{cases} \quad (4)$$

The parameters  $x_0$ ,  $x_1$ ,  $\bar{C}$ , and  $k$  from Eq. (4) be represented as in Eq. (5) and  $\bar{C}$  could be depend on the absorbing material and constants of the material itself where  $x$  could given as in Eq. (6).

$$x = \log(\rho/m_0c) = \log(\beta/\sqrt{1-\beta^2}) \quad (5)$$

$$\bar{C} = -\left(2 \ln\left(\frac{I}{\hbar\omega_p}\right) + 1\right) \quad (6)$$

In Eq. (6), the plasma frequency  $\omega_p$  is equal to  $\sqrt{N_e e^2 / \pi m_e}$  (Sternheimer et al., 1984). In the cases where compounds and mixtures, generated with more than one component are used as the stopping material, the stopping power of each component must be included in the calculation irrespective of the presence of

other components because the chemical binding energy established between the components have been accepted as negligible (Evans, 1955). For such cases, Bragg's rule was used and the stopping power has been obtained as given in Eq. (7) (Bragg and Kleeman, 1905).

$$\left(\frac{1}{\rho} \frac{dE}{dx}\right)_{compound} = \sum_i w_i \left(\frac{1}{\rho} \frac{dE}{dx}\right)_i \quad (7)$$

In Eq. (7),  $w_i$  represents the weight fraction of an element which contains  $N_i$  atoms and the

equation for  $w_i$  could be given as represented in Eq. (8) where  $A$  is the atomic weight [20].

$$w_i = \frac{N_i A_i}{\sum_j N_j A_j} \quad (8)$$

The other important parameter that also investigated in this study is the penetration distance of the charged particles in the absorber medium. The penetration distance,  $R$ , of a charged particle in a material is a concept that describes the thickness value in which the charged particles can readily penetrate within that substance. In the calculations of  $R$ , the Continuously Slowing Down Approximation (CSDA), which is the idea that the charged particle moving in a

substance loses its kinetic energy gradually and continuously, has been adopted. The CSDA does not accept the ideology that the kinetic energy of a charged particle is transmitted as the fractions of individual interaction events, unlike the most of the collision and radiation interactions. The equation given in Eq. (9) has been used for the CSDA range calculations (Seltzer and Berger, 1982).

$$R_{CSDA} = \int_0^{(E_K)_0} \frac{dE}{S_{total}(E)} \quad (9)$$

In Eq. (9),  $R_{CSDA}$  refers to the CSDA penetration distance of a charged particle within a substance where  $(E_K)_0$  is the initial kinetic energy of the charged particle and  $S_{total}(E)$  represents the total mass stopping power of the charged particle as a function of  $E_K$ , kinetic energy. For the heavy charged particles, which have been examined in this work, it could be said that they do not undergo radiative losses, they transmit a very small amount of energy in individual ionizing collisions and they often experience very small angular deviations as a result of flexible collisions. Consequently, their trajectories in the absorber material are generally straight in contrast to the light charged particles and their maximum penetration distance is almost equal to the  $R_{CSDA}$  (Evans, 1955).

The calculations of the mass stopping power of the investigated materials and the penetration distances of the charged particles on these materials have been done via computer aided simulation and calculation codes which are GEANT4 (Agostinelli et al., 2003) and MCNP (Goorley et al., 2013). The improvements in the IT sector and the advancements in the software development industry have provide countless benefits to many sectors likewise to the scientific researches. The powerful, accurate, effective in time and cost also user-friendly applications like abovementioned ones have been widely using for many applications such

as studies of high energy physics, theoretical and experimental studies of nuclear physics, accelerator physics, medical, space, military and many other fields with the acceptance in the literature. Due to their reliability, acceptance and accurate calculation skills, the 10.4.p02 version of the GEANT4 code and 6.1 version of the MCNP code have been used in this study. The charged particles have been selected as alphas, helium-3, tritons, deuterons and protons where their energy interval has been appointed from 1 MeV to 50 MeV. In all calculations via both codes, the same hardware and the operation system have been used to avoid any possible systematic crashes or complications that may affect the outcomes.

### 3. Results and Discussion

All the calculations for the materials and every charged particle condition have been carefully gathered and classified for better analyzes after the end of whole calculation process. The comparisons of the outcomes from both codes have been graphed for better visual analyses. Figures 1-5 show the particle penetration distance (cm) versus particle energy (MeV) graphs where Figures 6-10 show the material mass stopping power (MeVcm<sup>2</sup>/g) versus particle energy (MeV) graphs. In each graph, the results for all investigated charged particle situations via both codes have been given for the studied element and its oxide together.

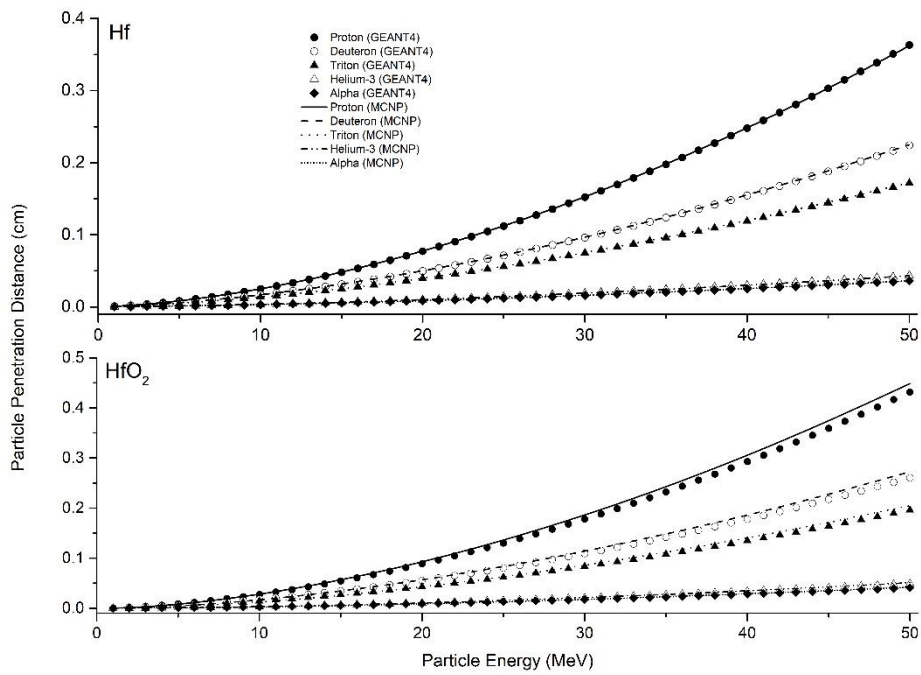


**Figure 1.** The particle penetration distance (cm) versus particle energy (MeV) graph for Hf and HfO<sub>2</sub>.

In Figure 1, the particle penetration distance calculation results have been given for the Hf and for the HfO<sub>2</sub> in the same frame where the upper half represents the Hf while lower half represents the HfO<sub>2</sub> results, respectively. As can be seen from the outcomes, the maximum penetrable particle is obtained as proton where the less penetrable particle could be given as

alpha for each material. In the calculations for the HfO<sub>2</sub>, a minor discrepancy between GEANT4 and MCNP results observed which also increases with the increase of incident particle energy. Even that, the obtained results show that the outcomes from both codes are in good consensus.

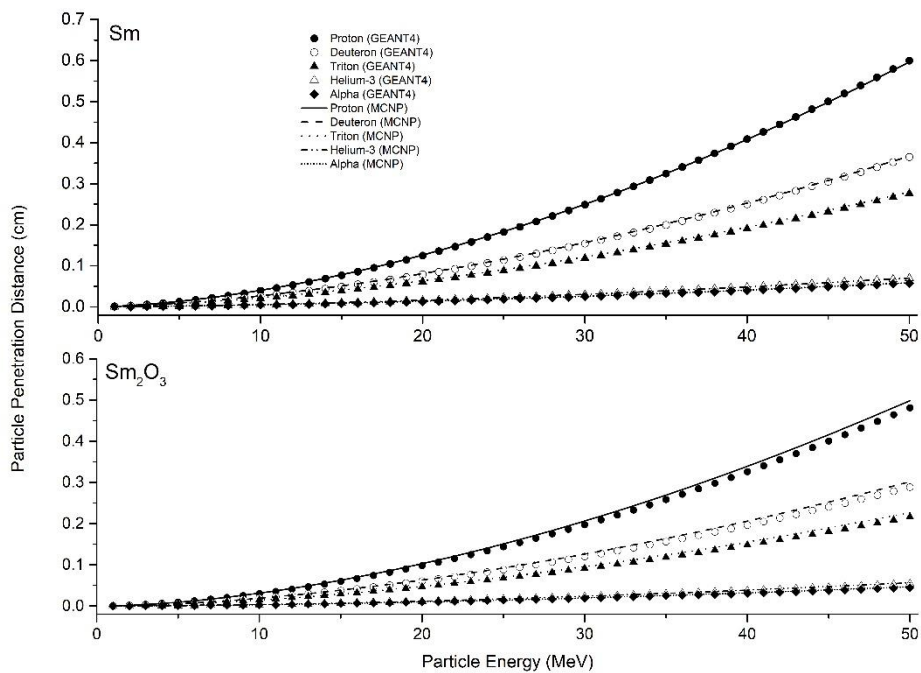


**Figure 2.** The same as Figure 1 but for Sm and Sm<sub>2</sub>O<sub>3</sub>.

The penetration distance results of the particles on Sm and Sm<sub>2</sub>O<sub>3</sub> have been given in

Figure 2 with a similar way which is done in Figure 1. Likewise, HfO<sub>2</sub> results, Sm<sub>2</sub>O<sub>3</sub>

calculations from the codes slightly differs from each other with the increase of incident particle energy where the MCNP calculations obtained higher with a small margin than the GEANT4 calculations. The ability of particles penetration through the materials has been

observed lowered for the  $\text{Sm}_2\text{O}_3$  compared to the Sm yet for both material the penetration distance for the investigated particles could be given in an order from higher to lower as proton, deuteron, triton,  $^3\text{He}$  and alpha.

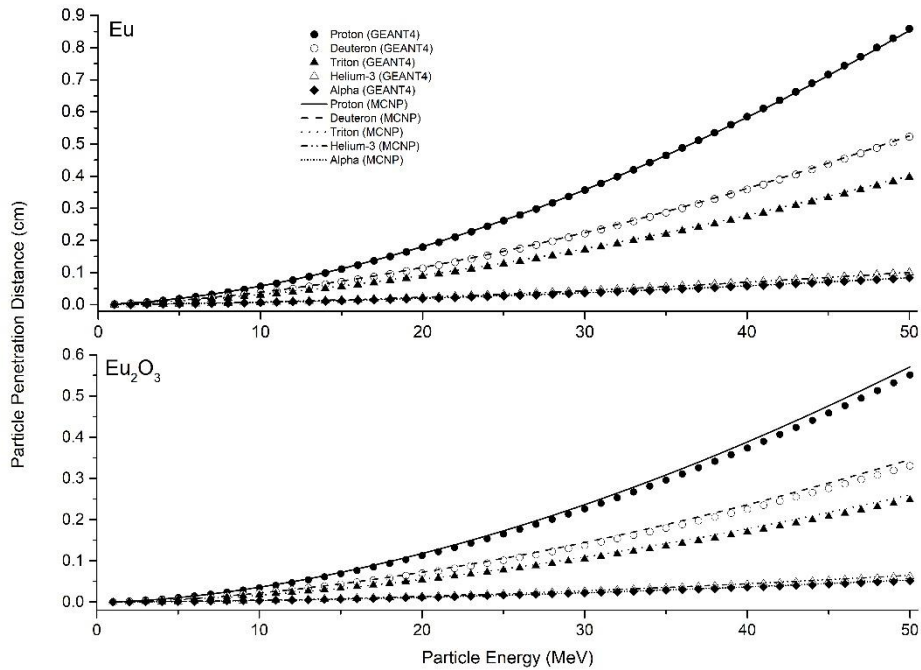


**Figure 3.** The same as Figure 1 but for Eu and  $\text{Eu}_2\text{O}_3$ .

The maximum particle penetration distance difference between the studied elements and their oxides has been obtained from the calculations accomplished for Eu and  $\text{Eu}_2\text{O}_3$  where the results have been graphed in Figure 3. For the Eu, the results obtained almost the same with each other from both codes where

a slight difference can be seen on the  $\text{Eu}_2\text{O}_3$  calculation results. This slight difference is mostly observed from the results of calculations performed for protons and is lowered for deuteron, triton,  $^3\text{He}$  and alpha particles, respectively.

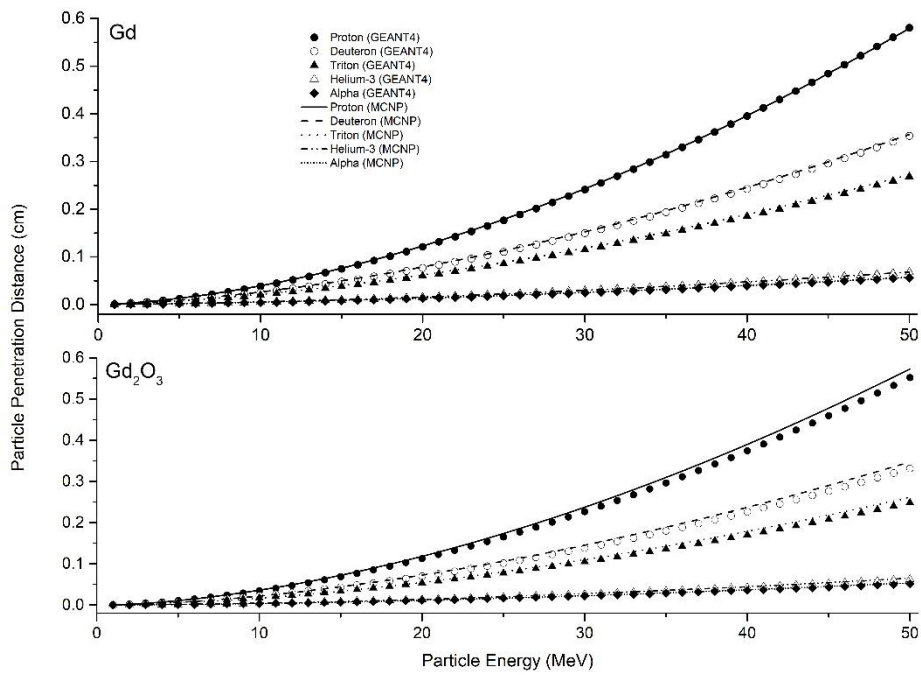


**Figure 4.** The same as Figure 1 but for Gd and Gd<sub>2</sub>O<sub>3</sub>.

The outcomes for Gd and Gd<sub>2</sub>O<sub>3</sub> have been given in Figure 4. Similar order of the particles for maximum penetration distance is

also valid for these materials likewise the slight difference of the outcomes between the codes for the oxide calculations.

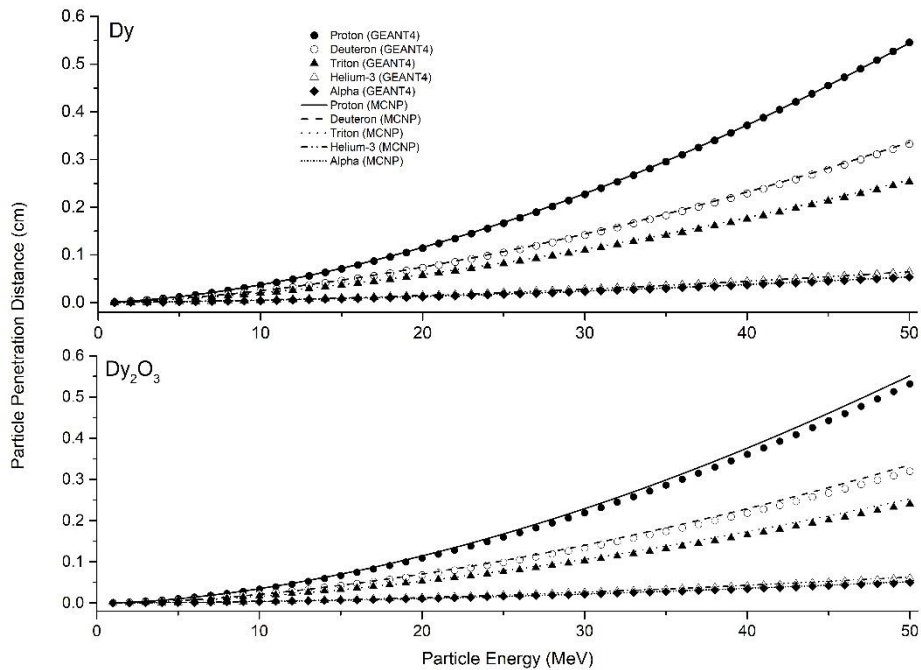


**Figure 5.** The same as Figure 1 but for Dy and Dy<sub>2</sub>O<sub>3</sub>.

In Figure 5, Dy and Dy<sub>2</sub>O<sub>3</sub> calculation results have been given where the minimum difference in the manner of particle penetration between the element and its oxide has been obtained on the lowest level with Gd and Gd<sub>2</sub>O<sub>3</sub>, given in Figure 4. For all the

materials shown in Figures 4 and 5, it is seen that the difference between the GEANT4 and MCNP results is slightly more evident than that of the materials shown in the other figures in the calculating distance of the deuteron particles.



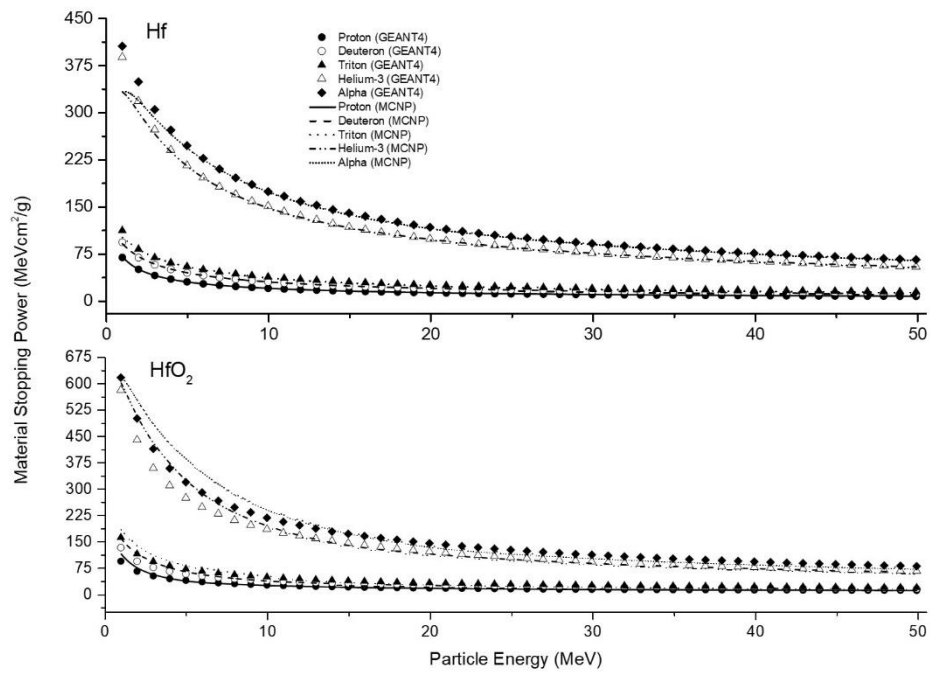


**Figure 6.** The material mass stopping power ( $\text{MeVcm}^2/\text{g}$ ) versus particle energy (MeV) graph for Hf and  $\text{HfO}_2$ .

The material mass stopping power versus particle energy for Hf and for the  $\text{HfO}_2$  have been represented in Figure 6. As expected, with the increase in the energy of charged particles, the stopping power decreases but not with a straight correlation. In accordance with the particle penetration distance calculation results, represented in Figure 1, the least mass stopping power value has been obtained for the protons and the maximum

value has been obtained for the alphas. For the energies below almost 3 MeV, a discrepancy between the GEANT4 and MCNP calculations has been observed in the calculation results performed for the alpha and  $^3\text{He}$  particles on Hf which does not exist for the  $\text{HfO}_2$  however a slight difference is observable for the calculations of protons on  $\text{HfO}_2$ .

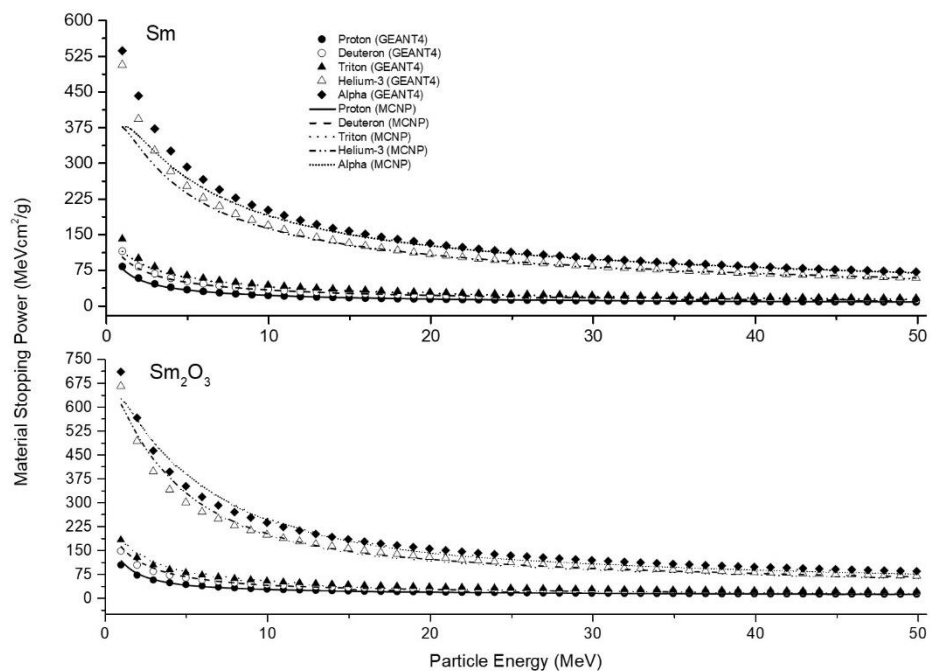


**Figure 7.** The same as Figure 6 but for Sm and  $\text{Sm}_2\text{O}_3$ .

The results obtained for Sm and  $\text{Sm}_2\text{O}_3$  have been given in Figure 7. With the increase in the incoming particle energy, the results from the codes have become more similar and the spot of difference which observed in the first

few results disappears. From the graphed results, it could be extracted that  $\text{Sm}_2\text{O}_3$  has better stopping characteristics rather than the Sm itself for the investigated charged particles and the energy interval in this study.

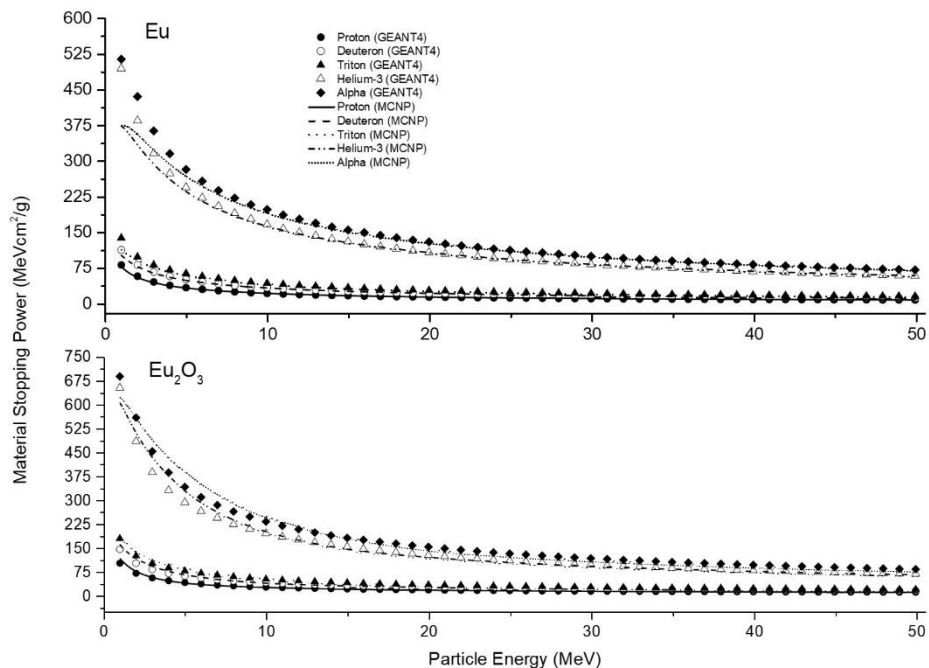


**Figure 8.** The same as Figure 6 but for Eu and  $\text{Eu}_2\text{O}_3$ .

Figure 8 represents the calculations performed for Eu and  $\text{Eu}_2\text{O}_3$  together. Likewise, the other performed mass stopping power calculations,

the difference in the first few points is observable but it is more clearly seen on the Eu calculations.

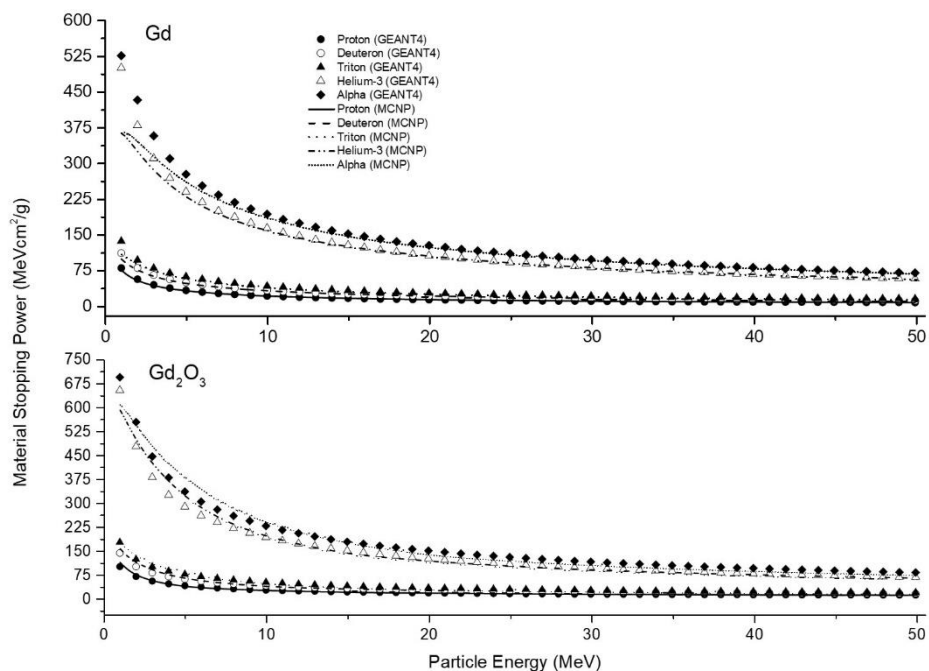


**Figure 9.** The same as Figure 6 but for Gd and  $\text{Gd}_2\text{O}_3$ .

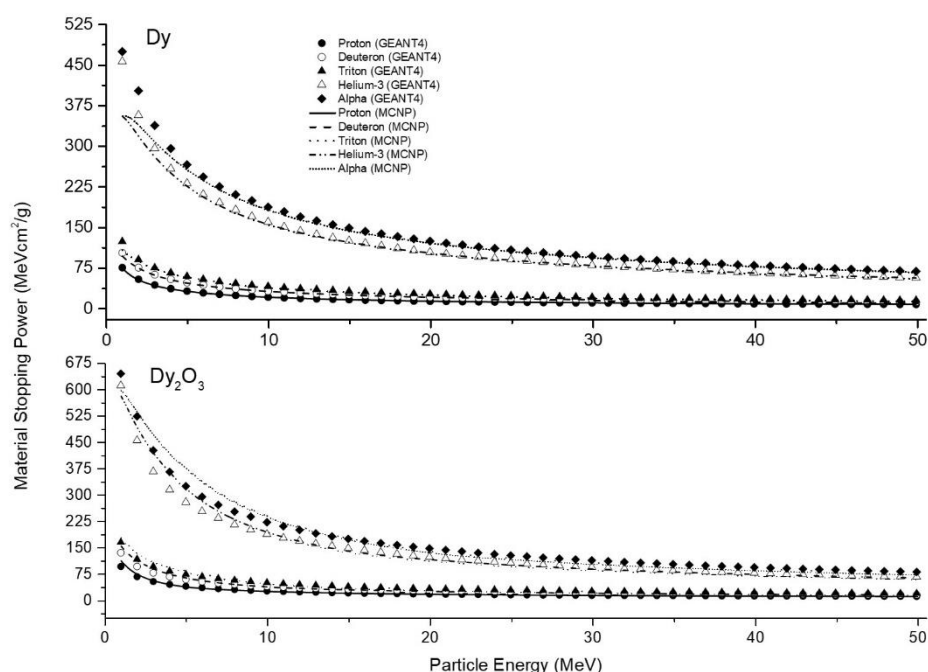


Figure 10. The same as Figure 6 but for Dy and Dy<sub>2</sub>O<sub>3</sub>.

From the outcomes of calculations which have been performed for Gd and Gd<sub>2</sub>O<sub>3</sub> represented in Figure 9 also for Dy and Dy<sub>2</sub>O<sub>3</sub> represented in Figure 10, it is possible to appoint a similar difference of the codes for the energy region below 3 MeV on the results that have been obtained for the elements. In both Figures 9 and 10, it is obvious that the mass stopping power values for the oxides have been achieved as higher than the elements.

#### 4. Conclusion

In this study, the calculations of mass stopping power and charged particle penetration distance have been performed for the materials which are considerable materials in the nuclear reactor control rod manufacturing. The brief outcomes of this study could be summarized as following.

- In this study, it is aimed to obtain the charged particle penetration distance and mass stopping power calculations in some nuclear reactor control rod materials. By doing so, it is aimed to better understand the interaction of the examined materials with charged particles and to contribute to the material development studies. In

addition, it is also aimed to compare the values obtained with the theoretical calculation and simulation programs used in the study and thus to examine the results of these commonly used programs in different charged particle situations, where a wide energy range of the particles, and to contribute to the development of the programs.

- The importance of having the mass stopping power and charged particle penetration distance values for the different materials has an undeniable importance since the information and knowledge on the mentioned topics have vital benefits for not only the material development studies but also for the different branches of science, engineering and industry.
- The most penetrable charged particle for all materials has been obtained as proton and the rest of the particles could be listed as deuteron, triton, <sup>3</sup>He and alpha considering the calculations performed with the same energetic particles.
- The increase in the particle energies causes an increase of the penetration distances and a decrease in the stopping

power as expected yet it should be pointed that the relation between the penetration distance and the stopping power is not straight proportional.

- The mass stopping power values of the studied materials for the investigated charged particles in this study have been obtained comparatively close for the Sm, Eu, Gd and Dy among elements and  $\text{Sm}_2\text{O}_3$ ,  $\text{Eu}_2\text{O}_3$ ,  $\text{Gd}_2\text{O}_3$  and  $\text{Dy}_2\text{O}_3$  among the oxides where the Hf and  $\text{HfO}_2$  has the lowest values. More investigations with higher energetic charged particles for these materials may provide more beneficial information which could be usable in different scientific and industrial applications.
- Detailed studies on the codes used in the calculations should be continued in order to be able to analyze the differences between the calculation results that can be seen in some of the materials examined.
- The computer aided applications like the ones employed in this study provide benefits for such calculations and many more. Even the simplifications they may provide and exist similar applications, a more accessible and user-friendly calculation tool for the mass stopping power and charged particle penetration distance may be more beneficial and usable for various applications and areas.

## 5. Acknowledgments

This work has been supported by the Süleyman Demirel University Scientific Research Projects Coordination Unit (Project No: 4599-D2-16).

## 6. References

Agostinelli, S., et al., 2003. "Geant4-a simulation toolkit". *Nuclear Instruments and Methods in Physics Research Section A: Accelerators, Spectrometers, Detectors and Associated Equipment*, 506(3), 250-303.

Artun, O. 2018a. "Calculation of the mass stopping powers of medical, chemical, and industrial compounds and mixtures". *Nuclear Technology and Radiation Protection*, 33(4), 356–362.

Artun, O. 2018b. "Estimation of Mass Stopping Power and Range via a New Computer Program X-PMSP". *Iranian Journal of Science and Technology, Transactions A: Science*, 43(2), 639–643.

Ashby, M. F., Smidman, M. 2010. "Materials for Nuclear Power Systems", Granta Material Inspiration.

Attix, F. H. 1986. "Introduction to Radiological Physics and Radiation Dosimetry", Wiley-Interscience, New York.

Becker, U., Coppi, B., Cosman, E., Demos, P., Kerman, A., Milner, R. 2008. "A perspective on the future energy supply of the United States: the urgent need for increased nuclear power", *MIT Faculty Newsletter*, XXI (2), 6-7

Bethe, H. A., Ashkin, J. 1953. "Passage of Radiations through Matter" in *Experimental Nuclear Physics Vol. 1*, ed. by E. Segre, John Wiley & Sons, New York.

Bozkurt, A., Sarpün, İ. H. 2018a. "Stopping Power of Protons for Energies and Materials of Therapeutic Importance Using Monte Carlo Simulations". *AIP Conference Proceedings*, vol. 1994, 040004.

Bozkurt, A., Sarpün, İ. H. 2018b. "Monte Carlo Calculated Stopping Power and Range of Alpha Particles in Water". *ICETAS-2018 Conference Papers, International Journal of Scientific & Engineering Research*, 9(8), 15–17.

Bragg, W. H., Kleeman, R. 1905. "On the  $\alpha$  particles of radium, and their loss of range in passing through various atoms and molecules". *The London, Edinburgh, and Dublin Philosophical Magazine and Journal of Science*, 10 (57), 318-340.

Evans, R. D. 1955. "The atomic nucleus", McGraw Hill Book Company, Inc., New York.

Goorley, J. T., et al., 2013. "Initial MCNP6 release overview-MCNP6 version 1.0", <https://laws.lanl.gov/vhosts/mcnp.lanl.gov/pd>

- f\_files/la-ur-13-22934.pdf, Access: October 5th, 2018.
- Groom, D. E., Klein, S. R. 2000. "Passage of particles through matter". *The European Physical Journal C*, 15(1-4), 163-173.
- IAEA (International Energy Agency), 1995. "Advances in control assembly materials for water reactors", IAEATECDOC-813, [https://inis.iaea.org/collection/NCLCollectionStore/\\_Public/26/077/26077302.pdf?r=1&r=1](https://inis.iaea.org/collection/NCLCollectionStore/_Public/26/077/26077302.pdf?r=1&r=1), Access: May 8<sup>th</sup>, 2019
- IAEA (International Energy Agency), 1996. "Absorber Materials, Control Rods and Designs of Shutdown Systems for Advanced Liquid Metal Fast Reactors", IAEATECDOC-884, [http://www.iaea.org/inis/collection/NCLCollectionStore/\\_Public/27/072/27072854.pdf](http://www.iaea.org/inis/collection/NCLCollectionStore/_Public/27/072/27072854.pdf), Access: May 8<sup>th</sup>, 2019
- IAEA (International Energy Agency), 2000. "Control assembly materials for water reactors: Experience, performance and perspectives", IAEATECDOC-1132, [http://www-pub.iaea.org/MTCD/Publications/PDF/te\\_1132\\_prn.pdf](http://www-pub.iaea.org/MTCD/Publications/PDF/te_1132_prn.pdf), Access: May 8<sup>th</sup>, 2019
- IAEA (International Energy Agency), 2017. "World Energy Outlook 2017", *OECD Publishing*, Paris, p 763.
- Kalcheva, S., Koonen, E. 2007. "Optimized Control Rods of the BR2 Reactor", *Open Report SCK-CEN-BLG-1054*, SCK-CEN, [http://publications.sckcen.be/dspace/bitstream/10038/814/1/cr\\_report.pdf](http://publications.sckcen.be/dspace/bitstream/10038/814/1/cr_report.pdf), Access: May 8<sup>th</sup>, 2019
- Paul, H., Schinner, A. 2003. "Empirical stopping power tables for ions from <sup>3</sup>Li to <sup>18</sup>Ar and from 0.001 to 1000MeV/nucleon in solids and gases". *Atomic Data and Nuclear Data Tables*, 85(2), 377-452.
- PRIS (Power Reactor Information System), <https://www.iaea.org/pris/>, Access: May 8<sup>th</sup>, 2019
- Seltzer, S. M., Berger, M. J. 1982. "Procedure for calculating the radiation stopping power for electrons". *The International Journal of Applied Radiation and Isotopes*, 33 (11), 1219-1226.
- Sternheimer, R. M., Berger, M. J., Seltzer, S. M. 1984. "Density effect for the ionization loss of charged particles in various substances". *Atomic Data and Nuclear Data Tables*, 30(2), 261-271.
- Tekin, H. O., Manici, T. 2017. "Simulations of mass attenuation coefficients for shielding materials using the MCNP-X code". *Nuclear Science and Techniques*, 28 (7), 95(1)-95(4).